

# Dose Distribution of $^{11}\text{C}$ Beams for Spot Scanning Radiotherapy

Eriko Urakabe\*<sup>a</sup>, Tatsuaki Kanai<sup>a</sup>, Mitsutaka Kanazawa<sup>a</sup>, Atsushi Kitagawa<sup>a</sup>, Koji Noda<sup>a</sup>, Takehiro Tomitani<sup>a</sup>, Mitsuru Suda<sup>a</sup>, Hideyuki Mizuno<sup>b</sup>, and Yasushi Iseki<sup>c</sup>

<sup>a</sup> National Institute of Radiological Sciences, 4-9-1 Anagawa Inage Chiba, 263-8555, Japan,

<sup>b</sup> Saitama Cancer Center, 818 Komuro Ina-machi Saitama, 362-0806, Japan, <sup>c</sup> Dept. of Energy Sciences, Tokyo Institute of Technology, Nagatsuta Midori Yokohama Kanagawa, 226-8502, Japan  
e-mail: urakabe@nirs.go.jp

## ABSTRACT

This paper describes the spot scanning with  $^{11}\text{C}$  beams for the Heavy Ion Medical Accelerator in Chiba (HIMAC). The concave-shaped irradiation field was optimized and the dose distribution was measured by 128-ch ionization chamber. Because of the wide momentum spread inherent in  $^{11}\text{C}$  beams, the dispersion caused from the beam line and the scanning magnets should be taken into account to calculate the dose distribution of  $^{11}\text{C}$  beams and their irradiated field. The reconstructed dose distribution is in good agreement with the experimental results.

**Keywords:**  $^{11}\text{C}$  Beam, Positron Emitter Beam, Dose Distribution, Spot Scanning, Heavy Ion Radiotherapy

## 1. INTRODUCTION

A scheme for spot scanning irradiation using  $^{11}\text{C}$  beams was developed in order to form and verify a three-dimensionally conformal irradiation field for heavy ion radiotherapy. Using positron emitter beams, such as  $^{11}\text{C}$  beams, a verification of the therapeutic irradiation can be accomplished by observing annihilation-pair gamma rays from the stopping position in the patient. A  $^{11}\text{C}$  beam produced by a projectile-fragmentation process, however, has relatively low intensity compared with that of a primary  $^{12}\text{C}$  beam (less than 1% of the primary beam). So, we have adopted the irradiation method with high beam utilization efficiency, spot scanning. In spot scanning at HIMAC, the position of each spot is controlled laterally by exciting a pair of scanning magnets and distally by installing PMMA plates (range shifter).

The beam line parameters for producing and selecting the  $^{11}\text{C}$  spot beam were optimized for the therapeutic irradiation. Since  $^{11}\text{C}$  spot beams have a wide momentum spread (2%), the aberration due to the momentum spread should be taken into account to calculate their dose distribution. Based on the spot beam envelope measured around the iso center, the dose distributions of  $^{11}\text{C}$  beams were calculated for each position determined by the scanning magnets and range shifter<sup>1</sup>. The irradiation field with a ‘concave’ shape, which is able to reduce the unnecessary dose for the case shown in Fig. 1, was designed in water phantom. The dose distribution of the spot beam and the irradiation volume were measured and it was found that the dispersion should be taken into account in the estimation of dose distribution.

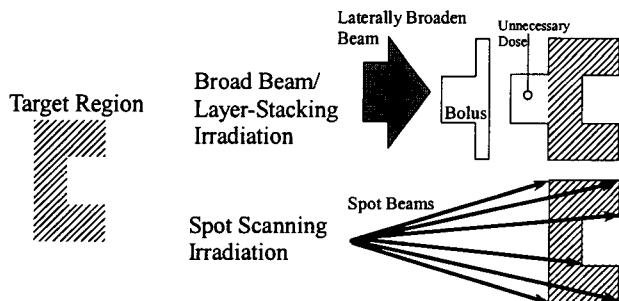


Fig. 1. Schematic view of the target and the irradiation regions. Spot scanning method can reduce the additional dose.

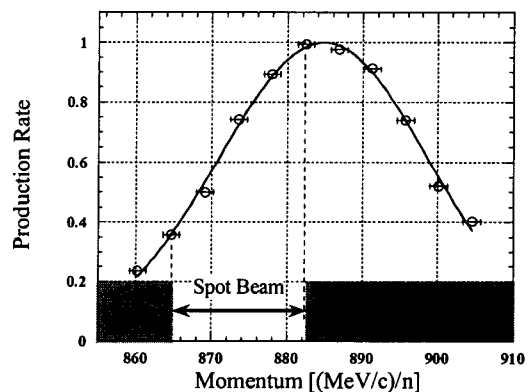


Fig. 2. Momentum distribution of  $^{11}\text{C}$  from  $^{12}\text{C}$  (430MeV/n) and Be (51mm).

## 2. DOSE ESTIMATION

### 2.1. Characteristics of $^{11}\text{C}$ Spot Beam

The  $^{11}\text{C}$  (346 MeV/n) beam produced by a projectile-fragmentation process through accelerated  $^{12}\text{C}$  (430 MeV/n) beams in a Be target (51mm thick) has the momentum distribution shown in Fig. 2. The yield of the  $^{11}\text{C}$  beam is less than 1% of that of the  $^{12}\text{C}$  beam under the full momentum acceptance (5%) of the beam line. The beam intensity and the width of distal falloff were used to select the momentum of the spot beam by the momentum slit and bending magnet, as indicated by a double headed arrow in Fig. 2. The central momentum of  $^{11}\text{C}$  was decided as 874 (MeV/n)/c, and its range of 200 mm in water is sufficient for treatment in head and neck region. The secondary beam line of HIMAC was designed to be doubly achromatic. The lateral size of the  $^{11}\text{C}$  spot beam is determined by the focusing condition.

### 2.2. Dose Estimation of $^{11}\text{C}$ Spot Beam

In order to deliver the desired dose to the irradiation volume, the depth dose and lateral dose distribution of the  $^{11}\text{C}$  spot beam were corrected by taking its wide momentum spread (2%) into account. The dose distribution at position  $d(x, y, z)$  is obtained by superposing the doses from all fraction with momentum  $P_i$ , as follows:

$$d(x, y, z) = \sum_i f(P_i) \cdot d^z(P_i, z) \cdot d^x(x, \sigma^x(P_i, z)) \cdot d^y(y, \sigma^y(P_i, z)) \quad (1)$$

where  $f$  is the momentum distribution as shown in Fig. 2 and  $d^z$  is the depth dose distribution of a monochromatic  $^{11}\text{C}$  beam calculated by Sihver's code<sup>2</sup>. Each beam fraction has a different lateral beam size as shown in Fig. 3 because of chromatic aberration of the lens system used in beam delivery. The lateral dose distributions of the monochromatic fraction  $d^x$ ,  $d^y$  are approximately estimated to be the Gaussian function  $G(x, \square)$ , where  $x$  and  $\square$  are its center and width. The widths of beam fractions were estimated with respect to the beam optics including chromatic aberration and the spread due to the multiple scattering<sup>1</sup>.

### 2.3. Irradiation Field Planning

In spot scanning, the spot beams should be designed so as to realize an irradiation field with a uniform dose and to minimize the extra dose outside the field. The dose of the irradiation field at the position,  $D(x, y, z)$ , is obtained by superposing the doses from all spot beams three-dimensionally:

$$D(x, y, z) = \sum_j w_j \cdot d(x_j, y_j, z_j), \quad (2)$$

where  $w_j$  is the weight of the dose delivered to  $j$ -th spot.

The spot weight was optimized by a least-square method to form a uniform irradiation field<sup>3</sup>, as shown in Fig. 4. Figure 4 (a) plots the contour lines of the irradiation field optimized for the target area shown by hatch. The lateral distribution at  $z=164$  and  $184$  mm is shown in Fig. 4 (b). The target regions at  $z=164$  and  $184$  mm are shown by solid and dashed double headed arrows, respectively. In the target region, the difference between the optimized dose and the prescribed one is within  $\pm 2\%$ .

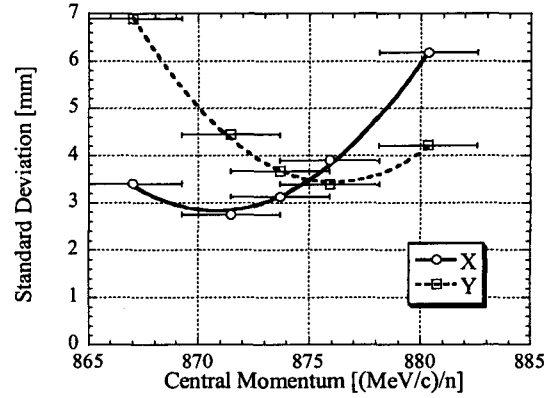


Fig. 3. Standard deviation of the lateral beam profile which depends on momentum and Be (51mm).

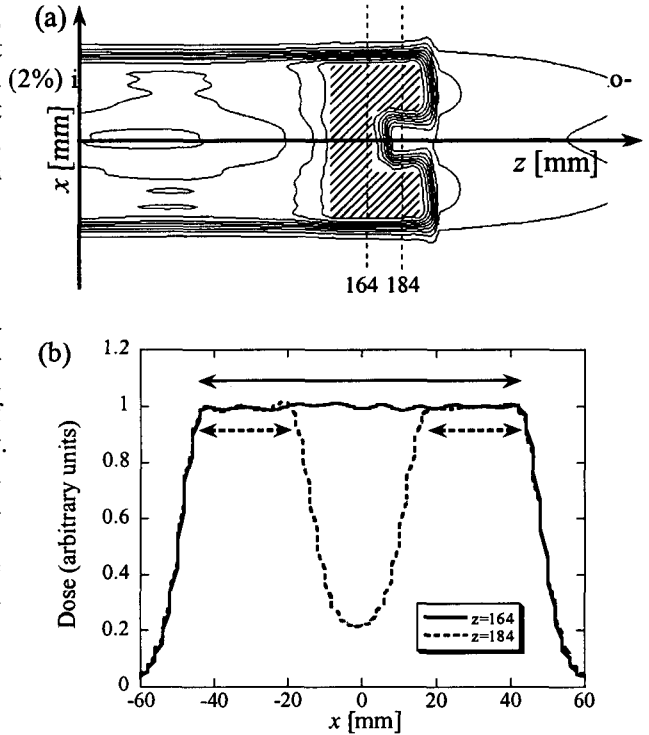


Fig. 4. The optimized irradiation field.

### 3. EXPERIMENTAL SETUP

The dose at each position was measured by a more efficient 128-ch ionization chamber (IC) to save time. Each ionization chamber consists of two parallel plates, with the capability for accurate measurements in the depth position. Each electrode ( $1.9 \times 1.9 \text{ mm}^2$ ) was made of gold-plated copper. For the horizontal and vertical measurements, the 128-ch signal electrodes were arranged as shown in Fig. 5. To get the faint signal in the low intensity beam, the gap between high voltage applied and signal electrodes was designed to be 10 mm. The 128-ch IC was operated with air of atmospheric pressure and enclosed in a water-resistant case of PMMA. 128-ch current signals integrated during irradiation are A/D converted and stored to a PC. For the dose measurement in water, the 128-ch IC was submerged into the water column, in which the depth position of the 128-ch IC could be changed by a motor drive. The thickness of the PMMA wall of the water column was 20 mm.

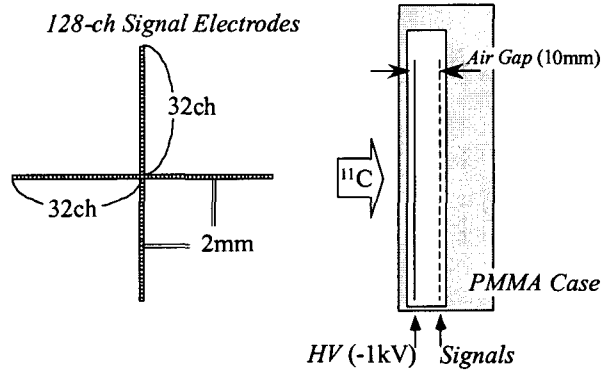


Fig. 5. Electrodes arrangement of 128-ch ionization chamber.

### 4. RESULTS

The centers of the lateral distribution  $x, y$  remained constant for a spot in Eq. (1), with which the dose distribution in the optimization procedure was calculated. The measured dispersion was  $\sim 0.07 \text{ m}$  due to the chromatic aberration, although the beam line was designed to be doubly achromatic. The excitation of the scanning magnets caused additional dispersion of momentum. For the spot of both ends, the dispersion caused from the scanning magnet is estimated to be  $0.05 \text{ m}$ . The dose distributions of the all spot and the irradiation field were recalculated including  $x(P_i, z), y(P_i, z)$  with two kinds of dispersion. Those of both ends ( $x = \pm 45 \text{ mm}$ ) and the central spots are shown in Fig. 6, from which and the asymmetry due to the dispersion can be seen. Irradiation by spot scanning for the optimized field was carried out. The dose distributions in the irradiation field were measured by the 128-ch IC. The open circles and open squares in Fig. 7 indicate the measured dose distribution at  $z=164, 184 \text{ mm}$ , respectively. Both measured results agreed well with the recalculated ones shown by the solid and dashed lines in Fig. 7.

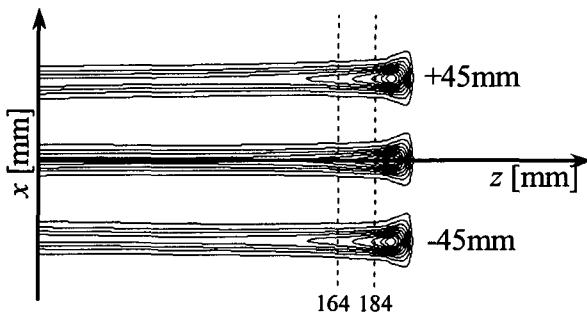


Fig. 6 The recalculated dose distribution of the deepest spot beams which indicates the effect of dispersion.

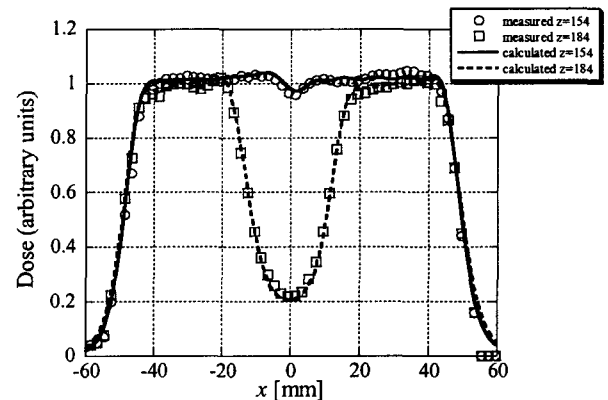


Fig. 7 Results of dose distribution of the irradiation field.

## 5. CONCLUSION

The concave-shaped irradiation field was optimized and the spot scanning with  $^{11}\text{C}$  beams were carried out. The dose distributions measured by the 128-ch ionization chamber and the water column were in good agreement with recalculated ones included the dispersion. In treatment planning, the effect of the dispersion should be included in order to optimize precisely the irradiation field in the spot scanning.

## REFERENCES

1. E. Urakabe et al. "Spot Scanning Using Radioactive  $^{11}\text{C}$  Beams for Heavy-Ion Radiotherapy", *Jpn. J. Appl. Phys.* **40**, pp. 2540-2548, 2001.
2. L. Sihver et al. "Depth-Dose Distributions of High-Energy Carbon, Oxygen and Neon Beams in Water", *Jpn. J. Med. Phys.* **18**, pp. 1-21, 1998.
3. A. Lomax, "Intensity Modulation Methods for Proton Radiotherapy", *Phys. Med. Biol.* **44**, pp.1-21, 1999.